horticulturae

MDPI

Article

The Aquaporin Gene *SbPIP1;2* Is Involved in Dormancy Release and Regulated Under Low Temperatures in *Lilium* 'Siberia'

Xuanmei Cai [1], Mingli Ke [1], Danfeng Ge [2,*] and Zhimin Lin [1,*]

[1] Fujian Academy of Agricultural Sciences Biotechnology Institute, Fuzhou 350003, China; caixuanmei@faas.cn (X.C.); keke1670@126.com (M.K.)
[2] Haixia Institute of Science and Technology, Fujian Agriculture and Forestry University, Fuzhou 350002, China
* Correspondence: dfge@fafu.edu.cn (D.G.); linzhimin@faas.cn (Z.L.)

Abstract

The dormancy of lilies is an important physiological process involving vernalisation and the differentiation and maturation of flower buds. We have cloned an aquaporin, *SbP1P1;2*, from the *Lilium* 'Siberia'. Subcellular localisation analysis indicates that it is a protein that is localised to the plasma membrane in *Nicotiana benthamiana*. VIGS-mediated transient silencing revealed that silencing the *SbPIP1;2* gene inhibited the development of lily flower buds, while those in the control group differentiated earlier to the anther primordia stage. Notably, the ABA levels in the control group had dropped significantly by day 63, suggesting that dormancy ended earlier than in the treatment group. The test plants' phenotype is characterised primarily by the fact that silencing the *SbPIP1;2* gene inhibits both flower bud development and root growth. The dormancy-to-sleep transition phase (PS vs. TS) was also the period during which the largest number of differentially expressed genes was observed. KEGG enrichment analysis indicates that starch and sucrose metabolic pathways are most active from the onset to the completion of dormancy release and that significant differences occur in several key genes within these pathways. These include alpha-trehalose-phosphate synthase (TPS), sucrose phosphate synthase (SPS), trehalase (TREH), fructokinase-1 (E2.7.1.1), beta-glucosidase (bglB), glycogen synthase (glgA), glucose-6-phosphate isomerase (GPI), and ectonucleotide pyrophosphatase/phosphodiesterase family members 1 and 3 (ENPP1/3). The discovery that aquaporins promote dormancy breaking in lilies is a highly successful case study for aquaporin research in flowers.

Keywords: *SbPIP1;2*; tobacco rattle virus; dormancy mechanism; RNA-seq; *Lilium*

Check for updates

Academic Editor: Dong Zhang

Received: 17 May 2026
Revised: 4 June 2026
Accepted: 10 June 2026
Published: 12 June 2026

Copyright: © 2026 by the authors. Licensee MDPI, Basel, Switzerland. This article is an open access article distributed under the terms and conditions of the Creative Commons Attribution (CC BY) license.

1. Introduction

Plant aquaporins (AQPs) are multifunctional membrane proteins that facilitate the transport of water as well as small molecules, including gases such as CO_2, nutrients such as boron and silicon, and reactive oxygen species (ROS) [1]. They are thought to have evolved from bacterial porins through gene duplication [2]. Currently, they are classified into four major subfamilies: plasma membrane intrinsic proteins (PIPs), NOD26-like intrinsic proteins (NIPs), tonoplast intrinsic proteins (TIPs), and small basic intrinsic proteins (SIPs) [3]. Compared with animals, plant AQPs possess a substantially larger repertoire of AQP isoforms, reflecting functional diversification rather than simple redundancy [4]. AQPs play a key role in various aspects of plant growth and development, including seed germination, root development, leaf growth, and the regulation of seed dormancy [5].

The diversity of plant AQPs is considerable. Genome-wide analyses have identified 35, 36, and 33 AQP-like sequences in *Arabidopsis thaliana*, maize, and rice, respectively [4]. Studies show that certain AQP subtypes can facilitate the movement of hydrogen peroxide (H_2O_2) across biological membranes [6]. Most PIPs primarily function as water channels, enabling dynamic changes in tissue water permeability [7]. AQP-mediated water transport is tightly regulated by multiple intracellular and environmental factors, including cytoplasmic conditions and ATP levels [8], phosphorylation, tetramerisation, pH, cations, reactive oxygen species, and plant hormones [9]. For instance, the phosphorylation-dependent switching between ion and water permeability in *AtPIP2* can be explained by the coupling between the gates of the four monomeric water channels with the central pore of the tetramer [10].

Transcriptomic analysis of the corolla tissues indicates that one *PIP2* gene is actively expressed, and its silencing leads to incomplete or delayed flower opening [11]. These findings suggest that *PIPs* in the roots of halophytes may control their response to salt stress by regulating cell-to-cell water transport (CCV) and phosphorylation [12]. In maize, *PIP2;5* is the primary factor that regulates cellular and tissue water conductance, and plays a key role in plant physiology under water-deficient conditions [13]. Similarly, members of the *PaAQP* family in mountain apricot, including *PaPIP1-3*, *PaPIP2-1*, and *PaTIP1-1*, exhibit high expression levels in flower buds during the dormancy and germination stages [14]. In *Litchi* buds, silencing of *LcPIP1:4a* induces a severe bud dormancy phenotype, accompanied by altered expression of regulatory genes such as *LcRAP2.4* and *LcPIP1:4*, further supporting the role of aquaporins in bud development and dormancy regulation [15].

Lilium spp. are commercially important ornamental bulbs whose growth and flowering are tightly controlled by dormancy, a physiological state that prevents premature sprouting under unfavorable conditions [16]. Dormancy release is a critical developmental transition in bulbs, marked by the reactivation and elongation of internal floral buds, accompanied by dynamic changes in endogenous hormones and visible morphological sprouting [17,18]. Key genetic regulators include the transcription factor *LoNFYA7*, which is essential for bud activation following dormancy [19], and *LdXERICO*, which modulates dormancy through ABA-dependent pathways [20]. Low-temperature treatment induces dormancy release through coordinated regulation of hormone signaling, carbohydrate metabolism, and cellular growth [21,22]. During this process, meristematic and parenchyma cells in the floral bud reinitiate division and expansion, supported by enhanced water transport that facilitates osmotic regulation and turgor maintenance. Although these physiological and genetic factors are recognized, the specific roles of AQPs in regulating water transport, osmotic balance, and metabolic activation during bulb dormancy release remain largely unexplored.

Based on our previous comparative transcriptome analysis of *Lilium* 'Siberia' bulbs cultivated at different altitudes following cold storage, *SbPIP1;2* was identified as a candidate AQP associated with dormancy release [23]. To investigate its biological function, we examined the role of *SbPIP1;2* during low-temperature-induced dormancy release using virus-induced gene silencing (VIGS) and transcriptome analysis. Our results demonstrate that silencing SbPIP1;2 delayed floral bud development and altered ABA and GA accumulation patterns. Furthermore, genes involved in starch and sucrose metabolism exhibited significant transcriptional changes following SbPIP1;2 silencing, suggesting a potential link between aquaporin-mediated water transport and metabolic activation during dormancy release.

2. Materials and Methods

2.1. Experimental Materials

Lilium hybrid 'Siberia' bulbs were cultivated in Yanping District, Nanping City, Fujian Province. In October, 2024, bulbs with a circumference of 8–10 cm were planted in greenhouses. Bulbs were harvested in April, 2025 when their circumference reached 16–20 cm, washed, and

brought back to the laboratory for TRV injection experiments. After treatment, bulbs were stored at 4 °C in substrate. Samples were collected at 35 (First stage, F), 63 (Second stage, S), and 130 (Third stage, T) days after planting and divided into *SbPIP1;2*-silenced (P) and control (T) groups, designated as PF and TF (35 days), PS and TS (63 days), and PT and TT (130 days). Each treatment group included three independent biological replicates, with each replicate consisting of three bulbs pooled together for downstream analyses.

2.2. Gene Clone

Total RNA was extracted from *Lilium* hybrid 'Siberia' bulb tissues using the RNAprep Pure Plant Kit for polysaccharide- and polyphenol-rich samples (TIANGEN, Beijing, China) according to the manufacturer's instructions, and first-strand cDNA was synthesized using oligo (dT) primers following the manufacturer's protocol (Vazyme, Nanjing, China). The full-length coding sequences of *SbPIP1;2* were amplified and sequenced (Sangon, Shanghai, China) using gene-specific primers (Table S1) based on recently published genomes [24]. The conserved domains of presumed proteins were predicted by using the Conserved Domain Database of NCBI (http://www.ncbi.nlm.nih.gov/Structure/cdd/wrpsb.cgi, accessed on 3 April 2026).

2.3. Virus-Induced Gene Silencing (VIGS) in Lilium

Virus-Induced Gene Silencing (VIGS) was performed to suppress the expression of *SbPIP1;2* in lily bulbs. Specifically, a 384 bp fragment of *SbPIP1;2* was cloned into the pTRV2 vector using ClonExpress® MultiS One Step Cloning Kit (Vazyme, Nanjing, China). The recombinant pTRV2-*SbPIP1;2* construct, together with empty TRV1 and TRV2 vectors, was transformed into *Agrobacterium tumefaciens* strain GV3101 (HeRui, Fuzhou, China). Single colonies were cultured overnight in LB liquid medium at 27 °C with shaking. Bacterial cells were collected by centrifugation and resuspended in infiltration buffer containing 10 mM $MgCl_2$, 200 μM acetosyringone, and 10 mM MES (pH 5.6). The suspension was adjusted to an OD_{600} value of 1.8–2.0. Equal volumes of TRV1 and either TRV2 or TRV2-*SbPIP1;2* cultures were mixed and incubated at room temperature in the dark for 3–6 h before infiltration. Three to five small holes were made at the basal plate of each bulb, followed by vacuum infiltration with the bacterial suspension (0.8 kPa, 15 min). After infiltration, bulbs were stored at 4 °C for subsequent phenotypic observation, RNA extraction, hormone analysis, and transcriptome sequencing.

2.4. Morphological Observations of Flower Bud Differentiation in Lilies

The apical portion of the flower bud was excised and placed in a 2 mL centrifuge tube. Samples were fixed in 1 mL FAA fixative (45% ethanol, 5% glacial acetic acid, and 5% formalin) followed by vacuum infiltration to facilitate penetration of the fixative. Fixation was carried out at room temperature for 2 days. The samples were subsequently dehydrated through a graded ethanol series (70%, 80%, 95%, fresh 95%, and 100%) for 1 h. T Dehydrated tissues were then cleared in ethanol–xylene mixtures at different volume ratios (xylene:alcohol = 2:1, 1:1, or 1:2) and left for 1 h. Finally, samples were infiltrated and embedded in molten paraffin for further sectioning and microscopic observation.

2.5. Transcriptomic Sequencing and Differential Gene Expression Analysis

Flower buds from wild-type and *SbPIP1;2*-silenced plants after cold storage at 35, 65, and 130 days were selected for transcriptomic sequencing. Total RNA was extracted and subjected to transcription sequencing (Maiwei Metabolic Biotechnology Co., Ltd., Wuhan, China). RNA extraction and cDNA synthesis were carried out using methods described in previous studies [25].

Poly(A)+ mRNA was enriched using oligo(dT) magnetic beads and subsequently fragmented into short sequences (Metware Biotechnology Co., Ltd., Wuhan, China). First-strand cDNA was synthesized using these RNA fragments as templates, followed by second-strand synthesis to generate double-stranded cDNA. The purified double-stranded cDNA was subjected to fragment size selection using magnetic beads. The resulting libraries were enriched by PCR amplification. The Fragment Analyzer (Agilent Technologies, Santa Clara, CA, USA) was used to determine the size of the library inserts. Qualified libraries were then subjected to pooling, depending on the target output data volume, and were sequenced on the Illumina platform (Metware Biotechnology Co., Ltd., Wuhan, China).

De novo transcriptome assembly was performed using clean reads obtained after quality control. Coding sequences (CDSs) were predicted from the assembled transcripts using TransDecoder (https://github.com/TransDecoder/, v5.3.0, accessed on 4 June 2026). Gene expression levels were quantified using RSEM (v1.3.1), and differentially expressed genes (DEGs) were identified with DESeq2 (v1.22.2) using the following thresholds: $|\log_2 \text{fold change}| \geq 1$ and adjusted p-value (FDR) < 0.05.

Functional enrichment analysis of DEGs was performed for both Gene Ontology (GO) terms and Kyoto Encyclopedia of Genes and Genomes (KEGG) pathways using the clusterProfiler package (v4.6.0). GO and KEGG annotations were obtained from the Gene Ontology Consortium and the Kyoto Encyclopedia of Genes and Genomes databases, respectively.

2.6. qRT-PCR Gene Expression Analysis

Total RNA was extracted using the Plant Total RNA Extraction Kit (Tiangen, Beijing, China). First-strand cDNA synthesis was performed according to the manufacturer's instructions. Gene-specific primers were designed using Primer6.0 software (Premier Biosoft International, Palo Alto, CA, USA; Table S1). Rbα-Tubulin was used as the internal reference gene.

qRT-PCR reactions were carried out using the AceQ Universal SYBR qPCR Master Mix Kit (Vazyme, Nanjing, China). Each 10 μL reaction mixture contained 100 ng cDNA template, 0.4 μL of each gene-specific primer (10 μM), 5.5 μL SYBR Green Master Mix, and nuclease-free ddH_2O to the final volume. Three biological replicates were analyzed for each sample, with three technical replicates performed per reaction. Relative gene expression levels were calculated using the $2^{-\Delta\Delta Ct}$ method [23]. Statistical analyses were conducted using SPSS 20.0 software (IBM Corp., Armonk, NY, USA).

2.7. Hormone Quantification and Statistical Analysis

The endogenous contents of gibberellin (GA) and ABA in lily bulbs were determined using plant GA and ABA enzyme-linked immunosorbent assay (ELISA) kits according to the manufacturer's instructions. Briefly, frozen samples were ground thoroughly, and the extracts were used for hormone quantification. Standard solutions and sample extracts were added to antibody-coated microplate wells, followed by incubation with horseradish peroxidase (HRP)-conjugated antibodies. After incubation at 37 °C for 30 min, the wells were washed five times with diluted washing buffer.

For color development, 50 μL of chromogenic solution A and 50 μL of chromogenic solution B were added to each well, followed by incubation at 37 °C in the dark for 10 min. The reaction was terminated by adding 50 μL of stop solution. Absorbance was measured at 450 nm using a SpectraMax 190 microplate reader (Molecular Devices, San Jose, CA, USA) within 15 min after stopping the reaction.

Hormone concentrations were calculated based on standard curves generated using serially diluted GA or ABA standards. The final hormone contents were corrected according to the dilution factor. Three biological replicates were analyzed for each treatment, and statistical analyses were performed using SPSS 20.0 software.

2.8. Subcellular Localization Analysis

The CDS of *SbPIP1;2* without the termination codon was amplified by PCR using specific primers (Table S1). The PCR products were then assembled into the linear expression vector pMD19-T by ClonExpress One Step Cloning Kit (Vazyme, Beijing, China). After digesting with *Bam*HI and *Sma*I, the PCR product was inserted into the modified vector pCAMBIA1300-35S-EGFP vector, and the constructed plasmid was transformed into *Agrobacterium tumefaciens* GV3101 (HeRui, Fuzhou, China) and transiently expressed in *Nicotiana benthamiana*. The fluorescence signal was observed using a LSM 880 microscope (Carl Zeiss AG, Oberkochen, Germany) for subcellular localization analysis, with GFP used as a nuclear marker.

3. Results

3.1. Molecular Characterization and Subcellular Localization of SbPIP1;2

The gene *SbPIP1;2* was successfully cloned from flower buds of *Lilium* 'Siberia' (Figure S1). *SbPIP1;2* possesses an open reading frame (ORF) of 867 bp, which encodes a 288-amino-acid protein. Conserved domain analysis using the NCBI database revealed that SbPIP1;2 contains the characteristic features of major intrinsic proteins (MIPs), including two highly conserved NPA motifs (Asn-Pro-Ala), hallmarks of AQPs. Subcellular localization analysis demonstrated that fluorescence signals were predominantly observed at the plasma membrane (Figures 1 and S2), supporting the conclusion that SbPIP1;2 is predominantly localized to the membrane in plant cells.

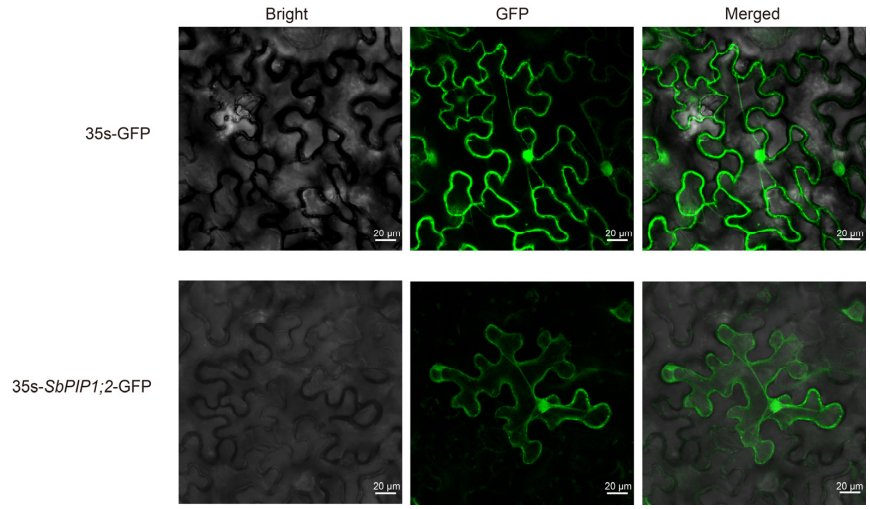


Figure 1. Subcellular localization of SbPIP1;2 in *Nicotiana benthamiana*. *SbPIP1;2* was fused to GFP and transiently expressed in *N. benthamiana* leaves under the control of the 35S promoter. Fluorescence was observed by confocal microscopy. **Top**: cells expressing GFP alone (35S-GFP) show bright-field, GFP fluorescence, and merged images, with GFP signal distributed throughout the cytoplasm and nucleus. **Bottom**: cells expressing *SbPIP1;2*-GFP (35S-*SbPIP1;2*-GFP) show bright-field, GFP fluorescence, and merged images, with fluorescence predominantly localized to the plasma membrane. Scale bars = 20 μm.

3.2. Morphological Observations During Flower Bud Differentiation

To investigate the potential role of *SbPIP1;2* in flower primordia, silence-inducing samples were induced using TRV-mediated VIGS. To evaluate the efficiency of TRV-mediated gene silencing in lily, the coat protein (CP) and movement protein (MP) regions of TRV were analyzed in flower buds. PCR results showed clear amplification in the gene-silenced lines, indicating that TRV successfully infected and spread systemically in the buds (Figure S3A). Consistently, *SbPIP1;2* transcript levels were significantly reduced in the silenced lines compared with controls, confirming effective TRV-mediated downregulation of the target gene

(Figure S3B). Silencing of *SbPIP1;2* significantly delayed floral primordia differentiation (Figure 2). In the control group, the differentiation of floral primordia began at 63 days (Figure 2B), and the differentiation stage of stamen primordia began to appear at 130 days (Figure 2C). In contrast, in *SbPIP1;2*-silenced plants, floral development was markedly delayed, with only perianth primordium differentiation observed at 130 days (Figure 2F).

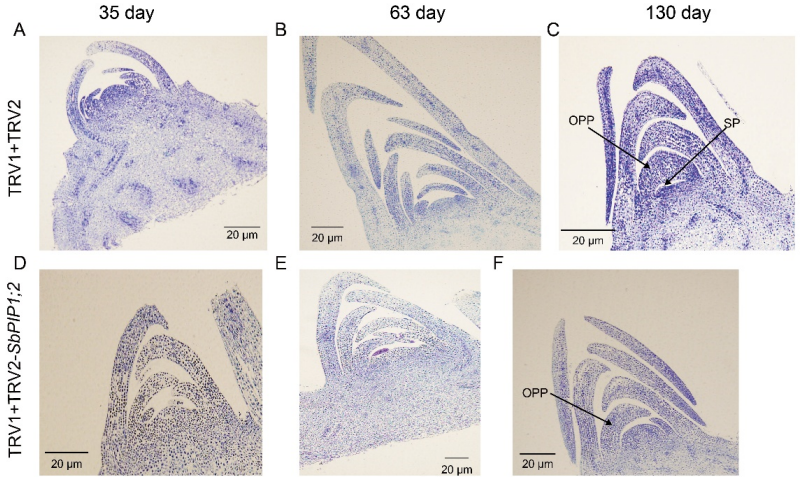


Figure 2. Morphological observations of flower buds in *Lilium* comparing the negative control and TRV2 + *SbPIP1;2* silenced bulbs during refrigeration at 4 °C. (**A**,**D**,**E**) Early stage of flower bud differentiation. (**B**,**F**) Outer perianth primordia (OPP). (**C**) Stamen primordia (SP). Panels (**A**–**C**) represent the control group (TRV1 + TRV2), and panels (**D**–**F**) represent the *SbPIP1;2*-silenced group (TRV1 + TRV2-*SbPIP1;2*). Scale bars = 20 μm.

3.3. Phenotypic Analysis of the TRV-Mediated Silencing of SbPIP1;2

Bulbs subjected to *SbPIP1;2* silencing failed to break dormancy until between 63 and 130 days, demonstrating a substantial delay in floral initiation. By 130 days, control bulbs (TRV1+TRV2) had developed more extensive and well-organized root systems than the silenced group (TRV1+TRV2-*SbPIP1;2*), highlighting the critical role of *SbPIP1;2* in coordinating dormancy release and early root development (Figure 3). Hormone analysis revealed that ABA levels steadily increased in the silenced bulbs, whereas GA accumulation was delayed relative to controls, suggesting that *SbPIP1;2* modulates hormonal regulation during dormancy release and early development (Figure S4). Notably, at 63 days, control bulbs exhibited reduced ABA and markedly higher GA levels compared with the silenced group, coinciding with the timing of dormancy break.

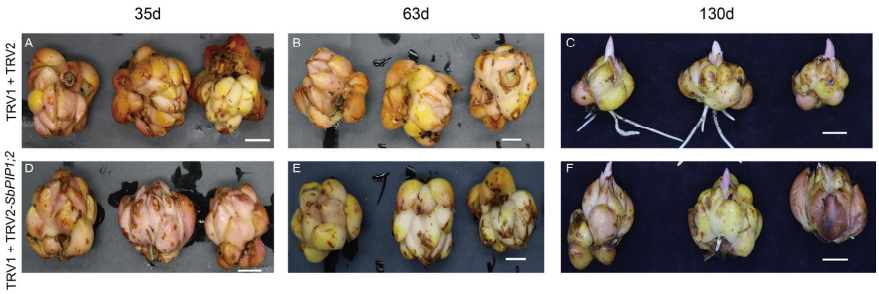


Figure 3. Phenotypic effects of *SbPIP1;2* TRV-mediated gene silencing in lily bulbs. Representative bulbs are shown at 35 (**A**,**D**), 63 (**B**,**E**), and 130 (**C**,**F**) days of low-temperature storage. Control bulbs (TRV1+TRV2; panels (**A**–**C**)) display normal floral bud differentiation and root development, whereas *SbPIP1;2*-silenced bulbs (TRV1 + TRV2-*SbPIP1;2*; panels (**D**–**F**)) exhibit delayed floral differentiation and altered bulb morphology, indicating that *SbPIP1;2* knockdown affects bulb development. Scale bars = 2 cm.

3.4. Differential Expression Analysis After TRV Silencing Treatment

Eighteen sequencing libraries were constructed from six samples with three biological replicates, which represented different stages of bulbil storage at low temperatures in *Lilium* 'Siberia'. After quality control, the number of clean reads per library ranged from 41 million to 57 million, corresponding to 6.15–10.4 Gb of clean bases per sample. De novo assembly of the RNA-seq data produced 236,546 transcripts with a mean length of 994 bp. After clustering, 132,926 unigenes were obtained for further analysis. Assessment of the transcriptome assembly using BUSCO indicated a high level of completeness (C:98.8% [S: 14.5%, D: 84.3%], F: 1.2%, M: 0.0%, n = 255), demonstrating that the assembly was sufficient for downstream analyses. Hierarchical clustering demonstrated strong separation among the sample groups, and principal component analysis (PCA) confirmed clear clustering of the gene-silenced (PF, PS, PT) versus control (TF, TS, TT) bulbs, reflecting consistent and reproducible transcriptional differences associated with *SbPIP1;2* knockdown (Figure S5). Differential gene expression analysis was performed across three stages of low-temperature treatment and dormancy release. Hierarchical clustering analysis revealed distinct expression patterns among the sample groups, indicating big transcriptional differences during dormancy release (Figure 4A). The PT vs. TF comparison had the highest number of DEGs (16,628; 7280 upregulated and 9348 downregulated), whereas the TT vs. TF comparison had the lowest (5214; 2567 upregulated and 2647 downregulated) (Figure 4B). The analysis revealed 599 DEGs shared across all three comparisons, while unique DEGs numbered 1139, 6141, and 5483 in PF vs. TF, PS vs. TS, and PT vs. TT, respectively (Figure 4C).

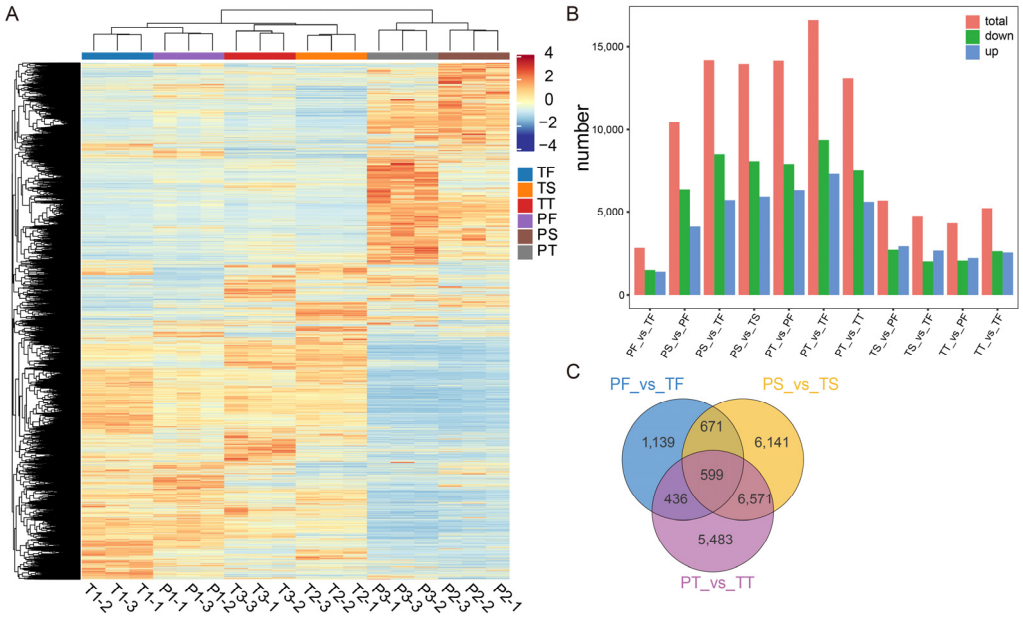


Figure 4. Transcriptome analysis of lily bulbs during dormancy release and TRV-mediated *SbPIP1;2* silencing. (**A**) Heatmap showing hierarchical clustering of differentially expressed genes (DEGs) across six sample groups (TF, TS, TT, PF, PS, PT) with three biological replicates each. The color scale represents Z-score normalized expression levels, with red indicating higher expression and blue lower expression. (**B**) Bar plot showing the number of DEGs for each pairwise comparison between gene-silenced and control groups. Blue bars indicate upregulated genes, green bars downregulated genes, and red bars total DEGs. (**C**) Venn diagram depicting shared and unique DEGs across the three comparisons (PF vs. TF, PS vs. TS, PT vs. TT), highlighting both common and stage-specific transcriptional responses during dormancy release.

Analysis of differentially expressed pathways across the three stages of dormancy release revealed that genes involved in starch and sugar metabolism were not significantly regulated at 35 days. In contrast, substantial differential expression emerged at 63 and 130 days, as indicated by KEGG enrichment analysis (Figure S6). GO enrichment further corroborated these results, showing a marked increase in genes associated with sucrose synthase activity, starch metabolism, and carbohydrate processing at 63 and 130 days (Figure S7). These transcriptional changes coincide with the observed dormancy-breaking phenotype, suggesting that activation of starch and sucrose metabolism is critical for the transition from dormancy to active growth. Specifically, key genes—including alpha-trehalose-phosphate synthase (*TPS*), sucrose phosphate synthase (*SPS*), trehalase (*TREH*), fructokinase-1 (*E2.7.1.1*), beta-glucosidase (*bglB*), glycogen synthase (*glgA*), glucose-6-phosphate isomerase (*GPI*), and ectonucleotide pyrophosphatase/phosphodiesterase family members 1/3 (*ENPP1_3*)—were significantly upregulated during stages 2 and 3. Consistently, analysis of starch and sugar metabolism revealed that soluble sugar content decreased markedly following *SbPIP1;2* silencing, correlating with delayed dormancy release and supporting a functional link between *SbPIP1;2*, carbohydrate metabolism, and dormancy regulation (Figure 5).

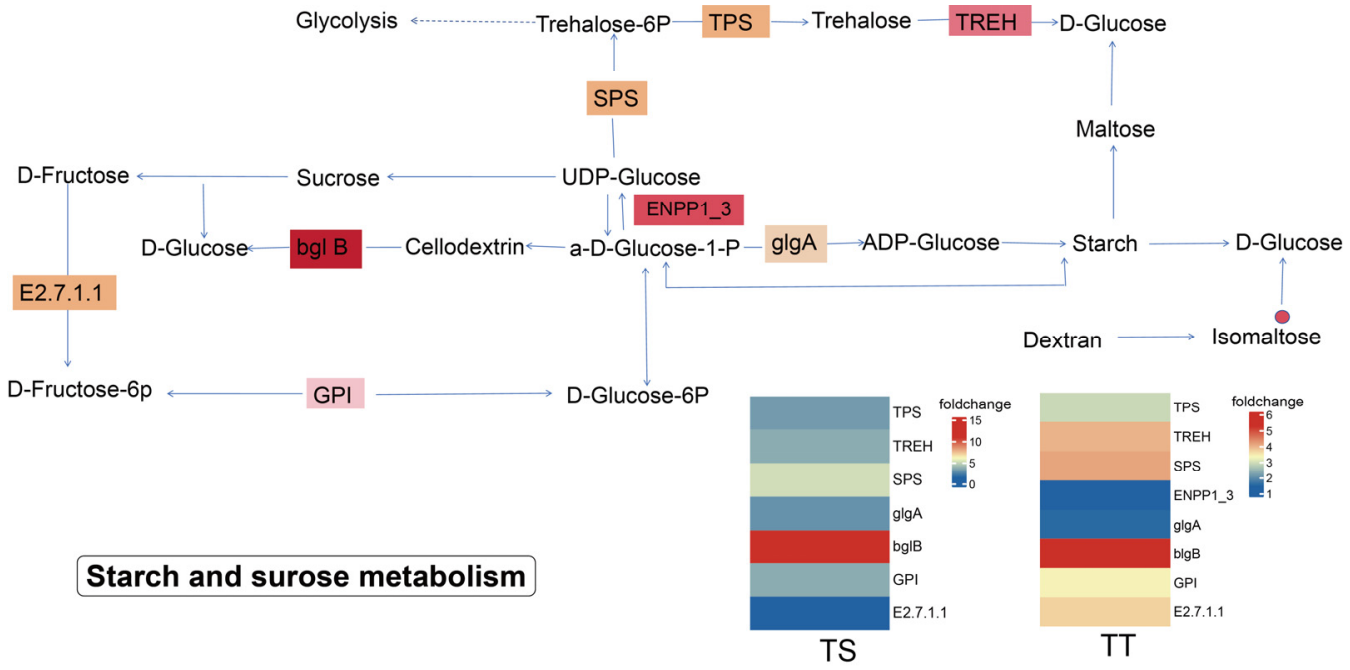


Figure 5. Differentially expressed genes in the starch and sucrose metabolism pathway. Metabolic network map showing key enzymes and intermediates involved in starch and sucrose metabolism. Circles indicate metabolites (red: upregulated), while the heatmaps represent fold changes of differentially expressed genes (DEGs) between PS (*SbPIP1;2*-silenced bulbs at 63 days) and TS (Control bulbs at 63 days) samples for each enzyme, including *TPS*, *TREH*, *SPS*, *ENPP1_3*, *glgA*, *bglB*, *GPI*, and *E2.7.1.1*.

4. Discussion

Dormancy release depends on the interplay of carbohydrate metabolism, hormonal balance, and enzymatic activity under low-temperature conditions [26–28]. Our study demonstrates that *SbPIP1;2*, a plasma membrane-localized aquaporin, plays a central role in regulating dormancy release in *Lilium* 'Siberia'. VIGS-mediated silencing of *SbPIP1;2* delayed floral primordia differentiation, postponed stamen development, and resulted in a marked delay in overall bud elongation. By 130 days, control bulbs exhibited fully differentiated flower buds and more developed root systems, whereas silenced bulbs

showed incomplete differentiation and altered morphology, highlighting the functional importance of *SbPIP1;2* during the dormancy-to-growth transition.

Low temperatures are often involved in the regulation of dormancy and can act to break dormancy in some seeds or bulbs through stratification or cold-induced physiological changes [29]. Storing bulb flower buds at low temperatures enhances their water content, whereas storing them at high temperatures inhibits water transfer between the central portion and lateral scales, leading to the abortion of flower bud development [30]. Most *Lilium* species have underdeveloped embryos at maturity, and low temperature is the primary environmental factor required to break bulb dormancy [31,32]. Studies suggest that treating oriental lilies at a low temperature affects both the elongation of their flower stems and the carbohydrate content of their bulbs [33].

Omics analysis indicated the involvement of water transport, osmotic balance, and metabolic activation during bulb dormancy release [21,22]. AQPs are a family of membrane proteins that facilitate the movement of water molecules and small polar solutes across biological membranes via osmosis [1,34]. Overexpression of the *PIP1* gene in tobacco has demonstrated that it significantly increases the water permeability of leaf protoplasts and the water conductance of cells [35]. At the cellular level, SbPIP1;2 is predominantly localized to the plasma membrane, consistent with its classification as a PIP-type aquaporin. The membrane localization of SbPIP1;2 suggests a primary role in facilitating cellular water transport, which is critical for maintaining turgor and enabling osmotic adjustments during dormancy release. Meristematic and parenchyma cells rely on controlled water flux to support cell division, elongation, and metabolic reactivation [36]. The delayed bud growth observed in *SbPIP1;2*-silenced bulbs is consistent with the potential reduced water transport capacity.

While plant hormone also involved in dormancy release [37], hormonal analysis supports a mechanistic link between *SbPIP1;2* activity and dormancy regulation. Silenced bulbs maintained higher levels of ABA and exhibited delayed GA accumulation compared with controls, coinciding with delayed bud elongation. This suggests that *SbPIP1;2* may modulate dormancy release in part by influencing hormone homeostasis, potentially by facilitating water-dependent signaling and metabolite distribution that affect ABA catabolism and GA biosynthesis. Such a connection aligns with previous findings that ABA maintains dormancy while GA promotes growth initiation, emphasizing the integration of water transport with hormonal control in dormancy release.

Transcriptome analysis further revealed that silencing *SbPIP1;2* affected the expression of genes involved in carbohydrate metabolism, including *TPS*, *SPS*, *TREH*, *glgA*, and *GPI*. Correspondingly, soluble sugar content was reduced in silenced bulbs, suggesting that *SbPIP1;2* may promote dormancy release by facilitating water and metabolite fluxes required for carbohydrate mobilization, energy availability, and hormonal signaling. Carbohydrate metabolism is crucial in this process, with sucrose acting as a key signal [38]. Our KEGG and GO enrichment analyses of transcriptomes from three stages of low-temperature vernalisation in seed tubers revealed significant variations in starch and sucrose metabolism, as well as in sucrose synthase activity. Significant differences in gene expression were particularly evident in the starch and sucrose metabolic pathways, including *TPS*, *TREH*, *SPS*, *ENPP1–3*, *glgA*, *blgB*, and *GPI*, suggesting the potential role of carbohydrate metabolism in dormancy release and floral differentiation. Interestingly, the transcriptomic data revealed that the timing of DEG activation corresponds closely with physiological observations: minimal differential expression occurred at 35 days, whereas substantial changes emerged at 63 and 130 days, aligning with the visible dormancy-breaking phenotype. This temporal pattern suggests that *SbPIP1;2* may function as a key early regulator in the dormancy-release cascade, potentially acting upstream of metabolic and hormonal reprogramming.

In summary, our findings reveal that *SbPIP1;2* is associated with physiological and molecular changes related to water transport, hormone balance, and carbohydrate metabolism during dormancy release. By delaying floral primordia differentiation, altering hormone accumulation, and reducing carbohydrate mobilization in silenced bulbs, *SbPIP1;2* emerges as a central component in the dormancy-release network. Nevertheless, the precise molecular functions of *SbPIP1;2* remain unclear. Further qRT-PCR validation of candidate genes, together with protein-level and functional analyses, will be necessary to clarify the downstream regulatory network and molecular mechanisms associated with *SbPIP1;2*-mediated dormancy release.

5. Conclusions

Vernalization and dormancy are key physiological processes in lily bulbs, yet their genetic regulation remains poorly understood. Our study identifies *SbPIP1;2*, a water channel protein, as a positive regulator of dormancy release. VIGS-mediated silencing of *SbPIP1;2* delayed bud growth, and transcriptomic analysis revealed altered expression of genes involved in sucrose and starch metabolism, consistent with the role of carbohydrate mobilization in breaking dormancy. These findings advance our understanding of the molecular mechanisms underlying lily dormancy and provide a foundation for future studies on aquaporins in lilies.

Supplementary Materials: The following supporting information can be downloaded at: https://www.mdpi.com/article/10.3390/horticulturae12060721/s1, Figure S1: (A) Gel electrophoresis of PCR-amplified *SbPIP1;2* open reading frame (ORF) from cDNA. Lane M, DNA marker (bp indicated); lane 1/2, PCR product showing the expected size (~867 bp). (B) Nucleotide sequence of the *SbPIP1;2* coding sequence (CDS); Figure S2: Subcellular localization of SbPIP1; 2-GFP in *Nicotiana benthamiana* epidermal cells. Confocal images show cells expressing *SbPIP1; 2*-GFP (bottom row) and free GFP control (top row). Columns represent bright-field, GFP fluorescence, and merged images. Scale bars: 20 μm for free GFP (control) and 50 μm for *SbPIP1;2*-GFP; Figure S3: TRV-mediated gene silencing in lily flower buds. (A) PCR detection of the coat protein (CP) and movement protein (MP) regions of TRV in lily flower buds. Lanes 1–2 represent TRV2-*SbPIP1; lanes 2* are infected (gene-silenced) lines, while lane 3 is a control (CK) buds. M, DNA marker. (B) Relative expression of SbPIP1;2 at 130 days after planting, showing reduced transcript levels in TRV2-*SbPIP1;2* lines compared with CK. Together, the CP and MP detection confirms successful infection and systemic spread of TRV vectors; Figure S4: Hormone dynamics in *SbPIP1;2*-silenced and control lily bulbs. (A) ABA concentration (ng/g) in control (TRV1 + TRV2) and *SbPIP1;2*-silenced (TRV1 + TRV2-*SbPIP1;2*) bulbs at 35, 63, and 130 days. (B) GA concentration (ng/g) in the same samples over time. Silenced bulbs exhibit elevated ABA and delayed GA accumulation compared with controls, consistent with the observed dormancy and developmental phenotypes; Figure S5: Principal component analysis (PCA) and sample correlation of RNA-seq libraries from Lilium bulbs under low-temperature treatment. (A) PCA plot showing clustering of 18 RNA-seq libraries across six groups: F (day 35), S (day 63), and T (day 130) for both control (TF, TS, TT) and treatment (PF, PS, PT). (B) Pearson correlation heatmap of all RNA-seq samples, with values ranging from 0.85 to 1.0. Darker red indicates higher correlation between samples, demonstrating strong reproducibility among biological replicates; Figure S6: KEGG enrichment analysis of differentially expressed genes (DEGs) among different dormancy-release stages and *SbPIP1;2*-silenced bulbs in Lilium 'Siberia'; Figure S7: Gene Ontology (GO) enrichment analysis of differentially expressed genes (DEGs) among different dormancy-release stages and *SbPIP1;2*-silenced bulbs in Lilium 'Siberia'; Table S1: List of gene-specific primers used for gene cloning.

Author Contributions: Conceptualization, Z.L.; methodology, X.C. and M.K.; software, D.G.; validation, X.C., D.G. and Z.L.; formal analysis, M.K.; investigation, Z.L.; resources, Z.L.; data curation, X.C. and M.K.; writing—original draft preparation, X.C. and Z.L.; writing—review and editing, D.G. and

Z.L.; supervision, Z.L.; project administration, Z.L.; funding acquisition, X.C. and Z.L. All authors have read and agreed to the published version of the manuscript.

Funding: This research was supported by Fujian Provincial Department of Science and Technology Provincial Public Welfare Research Project (2023R1025002, 2024R1026002).

Data Availability Statement: The original contributions presented in this study are included in the article/Supplementary Material. Further inquiries can be directed to the corresponding authors.

Conflicts of Interest: The authors declare no conflicts of interest.

References

1. Maurel, C.; Boursiac, Y.; Luu, D.T.; Santoni, V.; Shahzad, Z.; Verdoucq, L. Aquaporins in Plants. *Physiol. Rev.* **2015**, *95*, 1321–1358. [CrossRef]
2. Bezerra-Neto, J.P.; de Araújo, F.C.; Ferreira-Neto, J.R.C.; da Silva, M.D.; Pandolfi, V.; Aburjaile, F.F.; Sakamoto, T.; de Oliveira Silva, R.L.; Kido, E.A.; Barbosa Amorim, L.L.; et al. Plant aquaporins: Diversity, evolution and biotechnological applications. *Curr. Protein Pept. Sci.* **2019**, *20*, 368–395. [CrossRef]
3. Mukherjee, S.; Roy, S.; Corpas, F.J. Aquaporins: A vital nexus in H_2O_2-gasotransmitter signaling. *Trends Plant Sci.* **2024**, *29*, 681–693. [CrossRef]
4. Li, Y.; Wen, S.; Li, Z.; Liu, R.; Zhang, Z.; Li, Y.; Lyu, D.; Jian, H. The evolution of the aquaporin gene family and drought tolerance mechanisms in green plants. *Hortic. Res.* **2025**, *12*, uhaf209. [CrossRef] [PubMed]
5. Wang, Y.; Zhao, Z.; Liu, F.; Sun, L.; Hao, F. Versatile roles of aquaporins in plant growth and development. *Int. J. Mol. Sci.* **2020**, *21*, 9485. [CrossRef] [PubMed]
6. Bienert, G.P.; Chaumont, F. Aquaporin-facilitated transmembrane diffusion of hydrogen peroxide. *Biochim. Biophys. Acta* **2014**, *1840*, 1596–1604. [CrossRef]
7. Groszmann, M.; Osborn, H.L.; Evans, J.R. Carbon dioxide and water transport through plant aquaporins. *Plant Cell Environ.* **2017**, *40*, 938–961. [CrossRef] [PubMed]
8. Tan, X.; Xu, H.; Khan, S.; Equiza, M.A.; Lee, S.H.; Vaziriyeganeh, M.; Zwiazek, J.J. Plant water transport and aquaporins in oxygen-deprived environments. *J. Plant Physiol.* **2018**, *227*, 20–30. [CrossRef]
9. Kapilan, R.; Vaziri, M.; Zwiazek, J.J. Regulation of aquaporins in plants under stress. *Biol. Res.* **2018**, *51*, 4. [CrossRef]
10. Tyerman, S.D.; McGaughey, S.A.; Qiu, J.; Yool, A.J.; Byrt, C.S. Adaptable and multifunctional Ion-conducting aquaporins. *Annu. Rev. Plant Biol.* **2021**, *72*, 703–736. [CrossRef]
11. Herrera-Ubaldo, H. Masters of flower-bending: Aquaporins regulate flower re-opening. *Plant Cell* **2022**, *34*, 2578–2579. [CrossRef]
12. Gómez-Méndez, M.F.; Amezcua-Romero, J.C.; Rosas-Santiago, P.; Hernández-Domínguez, E.E.; de Luna-Valdez, L.A.; Ruiz-Salas, J.L.; Vera-Estrella, R.; Pantoja, O. Ice plant root plasma membrane aquaporins are regulated by clathrin-coated vesicles in response to salt stress. *Plant Physiol.* **2023**, *191*, 199–218. [CrossRef]
13. Ding, L.; Milhiet, T.; Parent, B.; Meziane, A.; Tardieu, F.; Chaumont, F. The plasma membrane aquaporin ZmPIP2;5 enhances the sensitivity of stomatal closure to water deficit. *Plant Cell Environ.* **2022**, *45*, 1146–1156. [CrossRef] [PubMed]
14. Li, S.; Wang, L.; Zhang, Y.; Zhu, G.; Zhu, X.; Xia, Y.; Li, J.; Gao, X.; Wang, S.; Zhang, J.; et al. Genome-wide identification and function of aquaporin genes during dormancy and sprouting periods of kernel-using apricot (*Prunus armeniaca* L.). *Front. Plant Sci.* **2021**, *12*, 690040. [CrossRef]
15. Tian, X.; Zhong, Z.Q.; Qi, Y.; Ma, M.M.; Yang, M.C.; Li, D.C.; Zhang, F.Y.; Wang, H.C.; Shen, J.Y.; Zeng, R.F.; et al. Two aquaporins, LcPIP1;4 and LcPIP1;4a, cooperatively regulate the onset of dormancy of the terminal buds in evergreen perennial litchi (*Litchi chinensis* Sonn.). *Hortic. Res.* **2025**, *12*, uhaf122. [CrossRef] [PubMed]
16. Mojtahedi, N.; Masuda, J.-I.; Hiramatsu, M.; Hai, N.T.L.; Okubo, H. Role of temperature in dormancy induction and release in one-year-old seedlings of *Lilium longiflorum* populations. *J. Jpn. Soc. Hortic. Sci.* **2013**, *82*, 63–68. [CrossRef]
17. Horvath, D.P.; Anderson, J.V.; Chao, W.S.; Foley, M.E. Knowing when to grow: Signals regulating bud dormancy. *Trends Plant Sci.* **2003**, *8*, 534–540. [CrossRef]
18. Ott, J.P.; Klimešová, J.; Hartnett, D.C. The ecology and significance of below-ground bud banks in plants. *Ann. Bot.* **2019**, *123*, 1099–1118. [CrossRef]
19. Pan, W.; Li, J.; Du, Y.; Zhao, Y.; Xin, Y.; Wang, S.; Liu, C.; Lin, Z.; Fang, S.; Yang, Y.; et al. Epigenetic silencing of callose synthase by VIL1 promotes bud-growth transition in lily bulbs. *Nat. Plants* **2023**, *9*, 1451–1467. [CrossRef]
20. Fan, X.; Zou, X.; Fu, L.; Yang, Y.; Li, M.; Wang, C.; Sun, H. The RING-H2 gene *LdXERICO* plays a negative role in dormancy release regulated by low temperature in *Lilium davidii* var. *unicolor*. *Hortic. Res.* **2023**, *10*, uhad030. [CrossRef]
21. Wang, W.; Su, X.; Tian, Z.; Liu, Y.; Zhou, Y.; He, M. Transcriptome profiling provides insights into dormancy release during cold storage of *Lilium pumilum*. *BMC Genom.* **2018**, *19*, 196. [CrossRef] [PubMed]

22. Fan, X.; Yang, Y.; Li, M.; Fu, L.; Zang, Y.; Wang, C.; Hao, T.; Sun, H. Transcriptomics and targeted metabolomics reveal the regulatory network of *Lilium davidii* var. *unicolor* during bulb dormancy release. *Planta* **2021**, *254*, 59. [CrossRef]
23. Fang, S.; Lin, M.; Ali, M.M.; Zheng, Y.; Yi, X.; Wang, S.; Chen, F.; Lin, Z. *LhANS-rr1*, *LhDFR*, and *LhMYB114* regulate anthocyanin biosynthesis in flower buds of *Lilium* 'Siberia'. *Genes* **2023**, *14*, 559. [CrossRef] [PubMed]
24. Sun, J.; Wang, X.; Wang, K.; Meng, D.; Mu, Y.; Zhang, L.; Wang, J.; Yao, G.; Guo, L. Genomic and epigenomic insight into giga-chromosome architecture and adaptive evolution of royal lily (*Lilium regale*). *Nat. Commun.* **2025**, *16*, 5617. [CrossRef]
25. Wang, S.; Yi, X.; Zhang, L.; Ali, M.M.; Ke, M.; Lu, Y.; Zheng, Y.; Cai, X.; Fang, S.; Wu, J.; et al. Characterisation and expression analysis of *LdSERK1*, a somatic embryogenesis gene in *Lilium davidii* var. *unicolor*. *Plants* **2024**, *13*, 1495. [CrossRef]
26. Huang, Y.; Song, J.; Hao, Q.; Mou, C.; Wu, H.; Zhang, F.; Zhu, Z.; Wang, P.; Ma, T.; Fu, K.; et al. WEAK SEED DORMANCY 1, an aminotransferase protein, regulates seed dormancy in rice through the GA and ABA pathways. *Plant Physiol. Biochem.* **2023**, *202*, 107923. [CrossRef]
27. Zhao, Y.; Pan, W.; Xin, Y.; Wu, J.; Li, R.; Shi, J.; Long, S.; Qu, L.; Yang, Y.; Yi, M.; et al. Regulating bulb dormancy release and flowering in lily through chemical modulation of intercellular communication. *Plant Methods* **2023**, *19*, 136. [CrossRef]
28. Huang, C.; Zhang, R.; Ye, C.; Xu, Y.; Li, Y.; Liang, K.; Wang, Y.; Jin, Q. Deciphering the ecodormancy and survival strategies of tropical water lily in northern subtropical environments. *BMC Plant Biol.* **2025**, *25*, 1422. [CrossRef] [PubMed]
29. Yan, A.; Chen, Z. The control of seed dormancy and germination by temperature, light and nitrate. *Bot. Rev.* **2020**, *86*, 39–75. [CrossRef]
30. Wang, Y.; Zhao, H.; Wang, Y.; Yu, S.; Zheng, Y.; Wang, W.; Chan, Z. Comparative physiological and metabolomic analyses reveal natural variations of tulip in response to storage temperatures. *Planta* **2019**, *249*, 1379–1390. [CrossRef]
31. Dhyani, A.; Phartyal, S.S.; Nautiyal, B.P.; Nautiyal, M.C. Epicotyl morphophysiological dormancy in seeds of *Lilium polyphyllum* (Liliaceae). *J. Biosci.* **2013**, *38*, 13–19. [CrossRef]
32. Li, Y.; Xin, Q.; Zhang, Y.; Liang, M.; Zhao, G.; Jiang, D.; Liu, X.; Zhang, H. Comparative metabolome analysis unravels a close association between dormancy release and metabolic alteration induced by low temperature in lily bulbs. *Plant Cell Rep.* **2022**, *41*, 1561–1572. [CrossRef]
33. Li, W.; Liu, X.; Lu, Y. Transcriptome comparison reveals key candidate genes in response to vernalization of oriental lily. *BMC Genom.* **2016**, *17*, 664. [CrossRef]
34. Markou, A.; Unger, L.; Abir-Awan, M.; Saadallah, A.; Halsey, A.; Balklava, Z.; Conner, M.; Törnroth-Horsefield, S.; Greenhill, S.D.; Conner, A.; et al. Molecular mechanisms governing aquaporin relocalisation. *Biochim. Biophys. Acta Biomembr.* **2022**, *1864*, 183853. [CrossRef]
35. Ding, X.; Iwasaki, I.; Kitagawa, Y. Overexpression of a lily *PIP1* gene in tobacco increased the osmotic water permeability of leaf cells. *Plant Cell Environ.* **2004**, *27*, 177–186. [CrossRef]
36. Alonso-Serra, J.; Cheddadi, I.; Kiss, A.; Cerutti, G.; Lang, M.; Dieudonné, S.; Lionnet, C.; Godin, C.; Hamant, O. Water fluxes pattern growth and identity in shoot meristems. *Nat. Commun.* **2024**, *15*, 6944. [CrossRef] [PubMed]
37. Shu, K.; Liu, X.D.; Xie, Q.; He, Z.H. Two faces of one seed: Hormonal regulation of dormancy and germination. *Mol. Plant* **2016**, *9*, 34–45. [CrossRef] [PubMed]
38. Pan, T.; Fan, X.; Li, M.; Yuan, H.; Sun, H. Sucrose synthase genes *LoSuSy* and *LoSuSy4* promote floral bud differentiation in lilies by degrading sucrose. *Plant Physiol. Biochem.* **2025**, *227*, 110010. [CrossRef]

Disclaimer/Publisher's Note: The statements, opinions and data contained in all publications are solely those of the individual author(s) and contributor(s) and not of MDPI and/or the editor(s). MDPI and/or the editor(s) disclaim responsibility for any injury to people or property resulting from any ideas, methods, instructions or products referred to in the content.